Clinical Pharmacokinetics (2025) 64:107–126
https://doi.org/10.1007/s40262-024-01460-6

ORIGINAL RESEARCH ARTICLE

A Pooled Pharmacokinetic Analysis for Piperacillin/Tazobactam Across Different Patient Populations: From Premature Infants to the Elderly

Daming Kong · Jason A. Roberts · Jeffrey Lipman · Fabio Silvio Taccone · Michael Cohen-Wolkowiez · Fekade B. Sime, et al. ***[full author details at the end of the article]***

Accepted: 7 November 2024 / Published online: 25 December 2024

Abstract

Background and Objectives The pharmacokinetics (PK) of piperacillin/tazobactam (PIP/TAZ) is highly variable across different patient populations and there are controversies regarding non-linear elimination as well as the fraction unbound of PIP (f_{UNB_PIP}). This has led to a plethora of subgroup-specific models, increasing the risk of misusing published models when optimising dosing regimens. In this study, we aimed to develop a single model to simultaneously describe the PK of PIP/TAZ in diverse patient populations and evaluate the current dosing recommendations by predicting the PK/pharmacodynamics (PD) target attainment throughout life.

Methods Population PK models were separately built for PIP and TAZ based on data from 13 studies in various patient populations. In the development of those single-drug models, postnatal age (PNA), postmenstrual age (PMA), total body weight (TBW), height, and serum creatinine (SCR) were tested as covariates. Subsequently, a combined population PK model was established and the correlations between the PK of PIP and TAZ were tested. Monte Carlo simulations were performed based on the final combined model to evaluate the current dosing recommendations.

Results The final combined model for PIP/TAZ consisted of four compartments (two for each drug), with covariates including TBW, PMA, and SCR. For a 70-kg, 35-year-old patient with SCR of 0.83 mg L^{-1}, the PIP values for V_1, CL, V_2 and Q_2 were 10.4 L, 10.6 L h^{-1}, 11.6 L and 15.2 L h^{-1}, respectively, and the TAZ values were 10.5 L, 9.58 L h^{-1}, 13.7 L and 16.8 L h^{-1}, respectively. The CL for both drugs show maturation in early life, reaching 50% at 54.2 weeks PMA. With advancing age, CL of TAZ declines to 50% at 61.6 years PMA, whereas CL of PIP declines more slowly, reaching 50% at 89.1 years PMA. The f_{UNB_PIP} was estimated as 64.5% and non-linear elimination was not supported by our data. The simulation results indicated considerable differences in PK/PD target attainment for different patient populations under current recommended dosing regimens.

Conclusions We developed a combined population PK model for PIP/TAZ across a broad range of patients covering the extremes of patient characteristics. This model can be used as a robust a priori model for Bayesian forecasting to achieve individualised dosing. The simulations indicate that adjustments based on the allometric theory as well as maturation and decline of CL of PIP may help the current dosing recommendations to provide consistent target attainment across patient populations.

1 Introduction

Piperacillin/tazobactam (PIP/TAZ) is an intravenous β-lactam/β-lactamase inhibitor combination product, which is frequently prescribed for moderate or severe infections in the intensive care unit setting due to its broad-spectrum antimicrobial activity against Gram-positive and Gram-negative bacteria [1–3]. Both PIP and TAZ are eliminated predominantly by the kidney with up to 68% of PIP and 80% of TAZ being excreted into urine as unchanged drugs [4].

Although PIP and TAZ have been in clinical use for more than three decades [5] and have been investigated in many studies, there is still debate around their pharmacokinetic (PK) properties. Various studies differ in included patient population and disease characteristics, which has translated

The members of PIP/TAZ Consortium are mentioned in "Acknowledgements".

Key Points

A single model is able to describe the pharmacokinetics of piperacillin and tazobactam in a broad population covering the extremes of age and weight.

Pharmacokinetic differences across subjects are mostly explained by a subject's age, bodyweight, and serum creatinine.

Current dosing recommendations of piperacillin and tazobactam do not accurately reflect age-related pharmacokinetic differences across subjects and result in inconsistent target attainment throughout life.

in various population PK model structures [6, 7]. Age, weight and creatinine clearance (CL_{CR}) of patients have been considered to explain part of the variability in the PK profile. However, different approaches have been used in the model development process, which has resulted in debate as to what covariates should be included and how to include them [1, 8–13]. There is also controversy about whether elimination of the drugs is saturable. Linear PK of PIP has been demonstrated in several studies [13–16]. On the other hand, some PK analyses reported non-linear elimination of PIP in healthy volunteers and patients with cystic fibrosis [3, 5, 17]. Although most studies reported that TAZ displays linear PK [18–20], evidence supporting non-linear PK of TAZ was found [2]. Another difficulty lies in prediction of unbound plasma concentrations (C_{UNB}) for PIP. Variability exists among the reported fraction unbound of PIP (f_{UNB_PIP}), leading to differing fractions from 70% to 78% being assumed in studies [15, 21, 22]. Given that the bactericidal activity of PIP depends on the proportion of time for which C_{UNB} is kept above the minimum inhibitory concentration (MIC) during a dosing interval ($fT_{>MIC}$) [23, 24], a reliable estimate for f_{UNB_PIP} is a requisite.

Therapeutic drug monitoring (TDM) plays an important role in optimising the PK target attainment of these drugs [25–27]. One of the most efficient ways to achieve individualised dosing is by using Bayesian forecasting based on an a priori population PK model. This technology can be facilitated by model-informed precision dosing (MIPD) software packages, such as InsightRx® (Insight Rx Inc., San Francisco, CA, USA) [28] and DosOpt (University of Tartu, Tartu, Estonia) [29]. However, the high variability and ongoing controversies on the PK of PIP/TAZ have resulted in numerous PK models, each specific to a different patient population. Clinicians, pharmacists, and pharmacology specialists have to understand the limitations of the models they use and switch models according to patient populations. This is a difficult task even for experts. It becomes easier and less critical when robust models suitable for a broad range of patients are available. In this study, we aimed to establish a single population PK model for PIP/TAZ based on a pooled dataset, which is broad enough to cover the extremes of patient characteristics. This model is expected to simultaneously describe the exposure of PIP and TAZ in different patient populations and facilitate routine clinical use.

2 Methods

2.1 Component Datasets

Pharmacokinetic studies of PIP/TAZ were identified through a PubMed search (until 20 November 2019), using search terms: "piperacillin AND pharmacokinetics [Title/Abstract]". We excluded studies in which patients received renal replacement therapy, extra-corporeal membrane oxygenation or non-intravenous administration of PIP/TAZ. Corresponding or senior authors of these included studies were invited for collaboration and sharing of anonymised data. Necessary institutional review board approval was attained for all included studies in the declarations from the original papers or from corresponding or senior authors.

Along with the observations, patient characteristics including postmenstrual age (PMA), postnatal age (PNA), sex, total body weight (TBW), height and serum creatinine (SCR) were extracted from component datasets. For patients other than neonates (PMA < 0.87 years), we assumed that their PMA was 40 weeks longer than the recorded PNA (years) [30]. For patients whose SCR records were all missing, we assumed they had standardised SCR values, as detailed below. If SCR records of a patient were partly missing, the missing values were supplemented by constant backwards propagation (next value carried backwards) based on the available SCR measurements.

A comprehensive check was conducted across component datasets. Contradictions in dosing records and questionable records of included patient characteristics were corrected in agreement with the corresponding or senior authors of the included studies.

2.2 Single-drug Pharmacokinetic Modelling

Single-drug population PK models for PIP and TAZ were separately developed by the same procedures. For each drug, one-, two- and three-compartmental PK models were compared to simultaneously fit all types of observations. Inter-individual variability (IIV) of typical parameter estimates was assumed to be log-normally distributed. A combined

proportional and additive residual-error model was used as a starting point to describe unexplained residual variability, which could be simplified when appropriate. Because of the possible difference between distributions of residual variability for different types of observations (total, unbound, and dried blood concentrations), coexistence of multiple combined residual-error models was also evaluated in both single-drug models. In addition, patient characteristics including TBW (kg), PMA (years), PNA (years), sex, height (m) and SCR (mg dL^{-1}) were tested as covariates for inclusion. Every covariate was tested in the PIP model in the same way as it was in the TAZ model. As the final step of single-drug modelling, non-linear elimination of PIP and TAZ was tested using an E_{max} function, where CL decreased when total plasma concentration increased.

2.3 Weight-Based and Compartmental Allometry

Based on previous studies [8, 9, 12, 15, 31, 32], TBW was a priori included in both single-drug models to correct PK parameters for size changes. Allometry scaling [33] was used to scale parameters to TBW with an exponent of 1 for volume terms (V_1, V_2, V_3) and an exponent of 0.75 for clearance terms (CL, Q_2, Q_3). Scaling was performed relative to a reference individual, a 70-kg male.

Compartmental allometry for inter-compartment clearance was tested in line with earlier work on propofol [34], dexmedetomidine [35], remifentanil [36] and vancomycin [30]. Specifically, inter-compartment clearance terms were scaled to the individual estimated size of the corresponding peripheral compartment to an exponent of 0.75. In Eq. 1, Q_i denotes individual estimates for inter-compartment clearance between the central and the *i*th compartment, V_i denotes individual estimates for peripheral volume of distribution for the *i*th compartment, and θ_{Vi} is the estimate for V_i of the reference individual.

$$Q_i \propto \left(\frac{V_i}{\theta_{Vi}}\right)^{0.75}, \quad i = 2, 3. \tag{1}$$

2.4 Maturation-Decline Function for Clearance

Based on the work by Lonsdale et al. [6] and Colin et al. [30], a function was tested to describe maturation of elimination clearance (CL) during early life and its subsequent decline with aging. Maturation of CL was modelled with a sigmoidal function (Eq. 2), in which MAT_{50} is the PMA in weeks when CL is increased to 50% and γ_1 is the shape factor defining the steepness of this non-linear relationship. In a similar way, a decline sigmoidal function was used to fit age-induced decline of CL (Eq. 3), in which DEC_{50} is the PMA or PNA at which CL gets reduced by 50% and γ_2 is the shape factor defining the steepness of this non-linear relationship.

$$\text{Maturation function} = \frac{\text{PMA}^{\gamma_1}}{\text{PMA}^{\gamma_1} + \text{MAT}_{50}{}^{\gamma_1}}, \tag{2}$$

$$\text{Decline function} = 1 - \frac{\text{age}^{\gamma_2}}{\text{age}^{\gamma_2} + \text{DEC}_{50}{}^{\gamma_2}}. \tag{3}$$

2.5 Testing Serum Creatinine as a Covariate in the Model

Serum creatinine was evaluated as a time-varying covariate on CL using an exponential function according to Eq. 4. θ_{SCR} defines the rate at which CL decreases with increasing SCR. To correct the estimate for θ_{SCR} for SCR values, a standardised SCR (SCR_{std}) value was used to centre SCR records. Different methods for standardising SCR were compared. First, the median and the mean value of SCR records were tested, respectively, as SCR_{std}. The reference SCR_{std} equations derived from the previous studies by Johansson et al. [37] and Colin et al. [30] were also included in this comparison. We also explored other approaches in which the "mfp : Multivariable Fractional Polynomials" package in R® (Version 1.5.2) was used to fit empiric SCR_{std} equations based on the age, weight and sex records derived from component datasets. The missing SCR records marked as 0 were assumed as SCR_{std} during the modelling process.

$$F_{SCR} = e^{-\theta_{SCR} \times \left(\text{SCR}(\text{mg dL}^{-1}) - \text{SCR}_{std}\right)}. \tag{4}$$

2.6 Combined Pharmacokinetic Modelling

A combined population PK model was established based on the single-drug models for PIP and TAZ. Given that PIP and TAZ have similar chemical structures and identical renal elimination pathways [22], they are expected to go through analogous PK processes in the human body. Similar or even identical information could be contained by a pair of parallel parameters that play the same role in the PK of PIP and that of TAZ. These relationships may be evident as a correlation between these parameters across models. Therefore, we tested the correlation within every pair of parallel PK parameters. For the fixed-effect parameters and the residual error terms, correlation between a pair of parallel parameters was tested by combining them into a single value. For the IIV terms, both covariance estimation and combining parameters (same/different magnitudes) were tested. After the evaluation of PK correlations was finished, a parallel linear and non-linear elimination was further tested for PIP.

2.7 Model Evaluation

The objective function value (OFV), Akaike information criterion (AIC), plots of IIV factor (ETA) versus covariate, goodness-of-fit (GOF) and the prediction- and variability-corrected visual predictive check (pvcVPC) [38] were used to determine whether a modification could be accepted into structural models and/or covariate model. In the structural changes of single-drug PK models and inclusion of covariate relationships, an additional parameter could be included when the OFV decreased by more than 3.84 points and observable improvements were shown in GOF and pvcVPC plots. Covariates were eligible for evaluation in the model if trends were visible in the graphic evaluation of ETA versus covariate relationships. During model development of the combined PK model, AIC instead of OFV was used to compare non-nested models resulted from covariance estimation and combining of parameters. For this, a reduction of one parameter was accepted with no AIC increase or apparent deterioration in GOF or pvcVPC observed. The GOF and pvcVPC were conducted hierarchically to avoid that the most populated subgroup dominates covariate analysis. As previously reported by Colin et al. [30], the following subgroups were created: pre-term and term newborns (PMA < 0.87 years), children and adolescents (PMA ≥ 0.87 years and aged < 18 years), adults (aged 18 years to < 65 years), elderly (aged 65 years to < 80 years), very elderly (aged ≥ 80 years), underweight adults (aged > 18 years and BMI < 18.5 kg m^{-2}) and obese adults (aged > 18 years and BMI > 30 kg m^{-2}). A model was accepted only when there was no obvious bias in GOF or pvcVPC across the subgroups. Parameter uncertainty was estimated by the covariance step in NONMEM or sampling importance resampling [39].

2.8 Evaluation of Current Dosing Recommendations

The current PIP/TAZ dosing guidelines approved by the European Medicines Agency (EMA) and the US Food and Drug Administration (FDA) were obtained from the summary of product characteristics (SmPC) for "Tazocin 4 g/0.5 g powder for solution for infusion" (Pfizer Ltd; available from http://www.medicines.org.uk; consulted on 19 April, 2024) and the label for "ZOSYN (piperacillin and tazobactam) for injection" (Pfizer Inc.; available from http://www.fda.gov; consulted on 19 April, 2024). The posologies extracted from the SmPC and the FDA label are shown in Table S1 and S2 of the Electronic Supplementary Material 4 (ESM4), respectively.

Probability of target attainment (PTA) at steady state for the SmPC- and the FDA-recommended dosing regimens were evaluated with Monte Carlo simulations. With the final combined model, 1000 virtual patients were simulated for each combination of age group, dosing guideline, and infusion duration. Six age groups were created according to EMA and FDA guidance [40–43]: neonates (aged < 28 days), infants (aged 28 days to < 2 years), children (aged 2 years to < 12 years), adolescents (aged 12 years to < 18 years), adults (aged 18 years to < 65 years) and elderly (aged ≥ 65 years). The PMA, PNA, TBW, and height of the virtual patients in each age group were fixed to the median values of the patients included in our study within the corresponding age group. Virtual patients were male with SCR values fixed to the SCR_{std}. All virtual patients received the highest recommended dose for their respective age, weight and sex, according to the SmPC and the FDA label. The influence of infusion duration on PTA was evaluated with intermittent infusions (30 min), extended infusions (half of the dosing interval), and continuous infusions.

As a beta-lactam antibiotic, PIP has a time-dependent bactericidal activity, which is defined by $fT_{>MIC}$. A $fT_{>MIC}$ of minimally 50% is required for clinical efficacy [2, 4]. As a higher target, a $fT_{>MIC}$ of 100% ($fT_{>MIC}$ 100%) was reported to be more beneficial for patients by preventing the possibility of bacterial regrowth [1]. Besides the prolonged exposure, an increase in PIP concentration was also found to lead to a rise in bactericidal activity until the PIP concentration exceeds four to five times the MIC [44]. Therefore, $fT_{>MIC}$ 100% and unbound PIP concentrations exceeding 4 times the MIC during the entire dosing interval ($fT_{>4*MIC}$ 100%) were used as PK/pharmacodynamics (PD) targets to evaluate the current dosing recommendations.

To evaluate TAZ exposure, the mean concentration of TAZ (C_{m_TAZ}) was calculated across age groups according to Eq. 5, where AUC_{ss_24h} denotes the area under the total TAZ concentration versus time curve for 24 h in steady state.

$$C_{m\_TAZ}\left(\text{mg L}^{-1}\right) = \frac{AUC_{ss\_24h}}{24}. \quad (5)$$

2.9 Software

The PK data were fitted using the FOCE-I estimation algorithm in NONMEM® (Version 7.5; Icon PLC, Dublin, Ireland). All models were managed with Pirana (Version 3.0.0; Princeton, New Jersey, USA). The GOF and pvcVPC were graphically assessed using the "tidyverse" package (Version 1.3.2; Wickham H. 2017) in R® (R Foundation for Statistical Computing, Vienna, Austria). Monte Carlo simulations were performed in NONMEM.

3 Results

3.1 Data

In total, 58 publications were identified through the PubMed search. After contacting the corresponding or senior authors by e-mail, we obtained individual-level data from 13 identified publications [7–9, 11–15, 32, 45–48] to generate a pooled dataset which covers a broad range of patients ranging from premature neonates [8] to very elderly people [11, 45, 46, 48], from underweight [11, 13, 46–48] to obese adults [7, 11, 13–15, 32, 45, 47, 48] and from critically ill patients with sepsis [11, 13, 15, 32, 46, 47] to febrile neutropenic patients with haematological malignancy [7]. The included PK data and patient characteristics are summarised in Table 1 and their distributions are shown in Figure S1 of the ESM1. In total, 3798 PIP concentrations and 1948 TAZ concentrations in different types of samples derived from 415 patients were included in this population PK analysis. The PIP observations comprised 2855 total plasma concentration (C_{TOT}) observations, 888 C_{UNB} observations and 55 observations of concentration in dried blood spot samples (C_{DBS}). However, for TAZ there were only C_{TOT} observations ($n = 1893$) and C_{DBS} observations ($n = 55$). The included patients consisted of 32 newborns, 127 children/adolescents, 74 elderly patients, 19 very elderly patients and 163 adults including 42 obese and 12 underweight. For 191 individuals, both PIP and TAZ concentrations were available. For 20 patients both C_{TOT} and C_{UNB} observations for PIP were available. For 28 patients both C_{TOT} and C_{DBS} observations for PIP and TAZ were available.

3.2 Single-Drug Pharmacokinetic Modelling

The developing hierarchy of single-drug models for PIP and TAZ is shown in Table 2. Generally, these two single-drug models were established through the same procedures. Both of them are 2-compartment models with linear elimination and identified covariates including TBW, PMA and SCR. Besides, PK alterations were observed for PIP in two component datasets. In the Sime et al. [7] study, which included patients with haematological malignancies, we found an elevated CL_{PIP} (+ 72.1%) and a lower V_{2_PIP} (− 48.3%). In the Sukarnjanaset et al. [11] study, a high f_{UNB_PIP} (100%) was observed. In the single-drug model for PIP, an additional set of proportional and additive residual errors is used for C_{UNB} observations, which is independent of that for C_{TOT} and C_{DBS} observations. For both drugs, non-linear elimination was tested but model fit was not significantly improved. We also tested non-linear protein binding of PIP using an E_{max} function. The estimated dissociation constant was high (854 mg L^{-1}) and the fit of the model to the data was not significantly improved (ΔAIC = − 0.12). Therefore, non-linear protein binding was not included in the single-drug model for PIP. More details about the model development process of single-drug models are described in the ESM2.

3.3 Combined Pharmacokinetic Modelling

The combined population PK model was established based on the final single-drug models for PIP and TAZ. We considered IIV terms, covariate fixed effects and residual error terms for combination across models. No apparent deterioration in model performance was caused by combining the θ_{SCR} of PIP and that of TAZ into one (ΔAIC = − 1.995), indicating that SCR influences CL_{PIP} in the same way as CL_{TAZ}. For every 0.20 mg dL^{-1} rise in SCR, CL_{PIP} and CL_{TAZ} both decrease by 6.7% according to the final combined model.

The maturation functions for the two drugs could be merged without significant changes to model fit (ΔAIC = − 0.38) with CL_{PIP} and CL_{TAZ} reaching 50% maturation at 54.2 weeks PMA (MAT_{50}). The decline functions could not be merged (ΔAIC = + 13.7) and in the final model, CL_{TAZ} declines by 50% at 61.6 years PMA (DEC_{50_TAZ}) whereas for CL_{PIP} this is 89.1 years PMA (DEC_{50_PIP}). The typical-for-PMA standardised CL_{PIP} (L h^{-1} 70 kg^{-1}) for all included patients is shown in Fig. 1A (solid line). For comparison, the maturation-decline function for PIP (dashed line), extracted from the pooled analysis by Lonsdale et al. [6] are also shown. As for TAZ, the typical-for-PMA standardised CL_{TAZ} (L h^{-1} 70 kg^{-1}) for all the included subjects with TAZ observations is shown in Fig. 1B.

Merging the ratio of C_{DBS} to C_{TOT} for PIP (f_{DBS_PIP}) and the one for TAZ (f_{DBS_TAZ}) together resulted in a worse fit (ΔAIC = + 8.82), revealing that significant differences existed between the estimates for this pair of parallel parameters. As estimated in the final combined PK model, concentrations of PIP and TAZ in dried blood spot samples are 63.2% and 55.2% lower, respectively, than those in plasma.

As for the other fixed-effect parameters of covariate-based and study-specific corrections, their estimates were slightly influenced although they were not enrolled into the correlation test. The f_{UNB_PIP} was estimated as 64.5% in the final combined PK model. In the patients derived from the study of Sukarnjanaset et al. [11], a higher f_{UNB_PIP} was observed ($f_{UNB\_Sukarnjanaset}$ = 100%). In addition, an increase by 73.2% and a decrease by 48.8% were sequentially identified for CL and V_2 in the Sime et al study, which included patients with haematological malignancies [7].

Later, we tested the correlation within every pair of parallel IIV terms. Ultimately, we could combine the IIV for PIP and TAZ for V_1, V_2 and Q_2, respectively, which produced the lowest AIC (ΔAIC = − 370.844) without interfering with the interpretation of the fixed-effect parameters.

Table 1 Summary of the component datasets. The distribution of patient characteristics and sampling and dosing records is summarised by the median and the range, with percentage of missing value in square brackets

Dataset	*N*	Patient population	% Males	PNA (y)[a]	PMA (y)[a,b]	TBW (kg)[a]	Height (m)	SCR (mg dL^{-1})[a]	No. of samples	No. of doses
Roberts et al. [15]	16	Critically ill patients with sepsis	75.0	35.5 (17.0–75.0)	36.3 (17.8–75.8)	80.0 (64.0–132.0)	1.76 (1.69–1.90)	0.67 (0.43–1.53)	23 (19–29)	4 (3–7)
Taccone et al. [44]	27	Critically ill patients with sepsis or septic shock	63.0	66.0 (36.0–89.0)	66.8 (36.8–89.8)	70.0 (49.0–100.0)	1.70 (1.55–1.85)	1.20 (0.50–4.10)	4 (4–5)	1 (1–1)
Cohen-Wolkowiez et al. [8]	32	Premature and term critically ill infants with suspected systemic infection	62.5	0.018 (0.003–0.164)	0.6 (0.5–0.9)	1.4 (0.5–4.0)	0.39 (0.29–0.53) [3.1%]	0.80 (0.30–2.00)	13 (8–30)	6 (4–10)
Sime et al. [7]	12	Febrile neutropenic patients with haematological malignancy	66.7	64.5 (53.0–79.0)	65.3 (53.8–79.8)	75.0 (53.0–103.0)	1.74 (1.53–1.84)	0.75 (0.50–1.08)	9 (6–9)	1 (1–1)
Tsai et al. [45]	9	Critically ill Australian indigenous patients with sepsis	55.6	43.0 (21.0–69.0)	43.8 (21.8–69.8)	73.1 (44.0–103.9)	1.72 (1.33–1.96)	0.81 (0.55–3.20)	16 (9–19)	3 (2–5)
Alobaid et al. [14]	37	Critically ill patients	56.8	49.0 (22.0–78.0)	49.8 (22.8–78.8)	90.0 (65.0–200.0)	1.67 (1.40–1.92)	0.96 (0.43–3.83)	5 (4–7)	5 (1–14)
De Cock et al. [9]	47	Critically ill children in ICU	44.7	2.8 (0.2–15.0)	3.6 (0.8–15.8)	14.0 (3.4–45.0)	0.92 (0.55–1.65)	0.21 (0.17–0.55)	9 (1–18)	5 (1–6)
Sukarnjanaset et al. [11]	50	Critically ill patients with sepsis	76.0	60.0 (22.0–94.0)	60.8 (22.8–94.8)	56.1 (38.0–122.8)	1.65 (1.40–1.84)	1.04 (0.27–3.64)	5 (3–5)	2 (1–4)
Dhaese et al. [30]	17	Critically ill patients	64.7	64.0 (19.0–78.0)	64.8 (19.8–78.8)	75.0 (55.0–100.0)	1.70 (1.60–1.95)	0.86 (0.39–3.88)	13 (10–13)	8 (3–27)
Udy et al [13]	48	Critically ill patients with sepsis	56.2	46.0 (18.0–78.0)	46.8 (18.8–78.8)	83.5 (53.0–175.0)	1.70 (1.50–1.92)	0.84 (0.43–2.08)	6 (4–6)	9 (1–29)
Felton et al [43]	17	Critically ill patients with pulmonary infection	52.9	53.6 (31.4–80.8)	54.3 (32.1–81.6)	75.0 (47.0–140.0)	1.74 (1.40–1.83)	0.75 (0.42–5.82)	12 (9–26)	7 (2–16)
Weinelt et al [46]	44	Critically ill patients	70.5	63.5 (23.0–82.0)	64.3 (23.8–82.8)	77.5 (50.0–124.0)	1.74 (1.50–1.98)	1.15 (0.50–4.70)	64 (28–104)	12 (5–16)
Thibault et al [12]	79	Infants and children ≥ 2 months to 6 years of age with infection	45.6	1.7 (0.2–6.3)	2.4 (0.9–7.0)	9.4 (3.8–27.6)	[100%]	0.41 (0.24–0.78) [3.8%]	4 (2–8)	16 (2–70)

ICU intensive care unit, *PMA* postmenstrual age, *PNA* postnatal age, *SCR* serum creatinine, *TBW* total body weight

[a]Covariate values at the time of inclusion into the study are shown. During the modelling, these covariates were considered to be time-varying and their entire time course was taken into account

[b]PMA in years (y) was derived from component datasets or assumed to be PNA plus gestational age with a default of 40 weeks for subjects with missing gestational age

Table 2 The developing hierarchy of single-drug population pharmacokinetic models

No.	Reference model	Description	OFV	ΔOFV	MAT_{50} (yr)	γ_1	DEC_{50} (yr)	γ_2	θ_{SCR}	IIV V_1 (%)[a]	IIV CL (%)[a]	IIV V_2 (%)[a]	IIV Q_2 (%)[a]
Single–drug population pharmacokinetic model for PIP													
1		A 2-compartment model with fraction unbound (f_{UNB_TAZ}) and ratio of C_{DBS} to C_{TOT} (f_{DBS_TAZ})	29,044.4							286	275	383	84.9
2	1	Allometry	27,726.4	− 1318.0						44.0	85.0	80.1	90.8
3	2	PMA-induced maturation of CL (F_{MAT}; Eq. 16)	27,526.2	− 200.2	0.844	4.62				41.5	63.4	77.8	53.2
4	3	PMA-induced decline of CL (F_{DEC}; Eq. 17)	27,475.1	− 51.1	1.08	3.46	82.3	0.961		40.8	56.7	76.2	52.9
5	4	SCR on CL (Eq. 4) with SCR_{std} as a non-linear function of PMA	27,268.8	− 206.3	1.07	3.39	92.7	1.48	0.357	41.1%	47.4	75.2	46.9
6	5	Compartmental allometry	27,236.6	− 32.2	1.07	3.39	92.8	1.49	0.357	38.2	47.6	78.2	20.6
7	6	Removal of IIV of Q2	27,237.1	+ 0.5	1.07	3.39	92.8	1.48	0.357	37.9	47.4	79.2	0 FIX
8	7	Study of Sime et al. [7] as a covariate on CL	27,219.4	− 17.7	1.07	3.35	86.5	1.51	0.354	37.9	46.0	79.2	0 FIX
9	8	Study of Sime et al. [7] as a covariate on V2	27,212.1	− 7.3	1.07	3.35	85.6	1.49	0.354	37.9	46.1	77.9	0 FIX
10	9	f_{UNB_PIP} exclusive to the Sukarnjanaset et al. [11] study ($f_{UNB\_Sukarnjanaset}$)	27,155.8	− 56.3	1.09	3.32	92.8	1.30	0.350	36.6	44.0	78.2	0 FIX
11	10	Addition of residual errors for unbound concentration	27,114.5	− 41.3	1.09	3.32	84.8	1.63	0.343	36.0	43.7	76.2	0 FIX
Single-drug population pharmacokinetic model for TAZ													
12		A 2-compartment model with ratio of C_{DBS} to C_{TOT} (f_{DBS_TAZ})	7303.7							706	359	410	68.6
13	12	Allometry	6784.5	− 519.2						49.6	102.3	77.5	50.0

Table 2 (continued)

No.	Reference model	Description	OFV	ΔOFV	MAT_{50} (yr)	γ_1	DEC_{50} (yr)	γ_2	θ_{SCR}	IIV V_1 (%)[a]	IIV CL (%)[a]	IIV V_2 (%)[a]	IIV Q_2 (%)[a]
14	13	PMA-induced maturation of CL (F_{MAT}; Eq. 16)	6688.2	− 96.3	0.774	4.95				48.7	71.2	74.9	49.9
15	14	PMA–induced decline of CL (F_{DEC}; Eq. 18)	6613.6	− 74.6	0.990	3.56	55.7	2.59		47.8	56.5	73.9	53.5
16	15	SCR on CL (Eq. 4) with SCR_{std} as a non-linear function of PMA	6489.2	− 124.4	1.01	3.35	61.6	2.06	0.343	47.7	43.6	68.6	49.0
17	16	Compartmental allometry	6481.2	− 8.0	1.01	3.35	61.6	2.02	0.350	40.8	43.2	70.0	51.0

C_{DBS} drug concentration in dried blood samples, *CL* elimination clearance, C_{TOT} total plasma concentration, DEC_{50} the postmenstrual age when elimination clearance decreases to 50% of the maximum value, *IIV* inter-individual variability, MAT_{50} the postmenstrual age when elimination clearance increases to 50% of the maximum value, *OFV* objective function value, *PIP* piperacillin, *PMA* postmenstrual age, Q_2 inter-compartment clearance, *SCR* serum creatinine, SCR_{std} standardised SCR, *TAZ* tazobactam, V_1 central volume of distribution, V_2 peripheral volume of distribution, γ_1 shape factor for maturation of CL, γ_2 shape factor for decline of CL, θ_{SCR} effect coefficient of serum creatinine on elimination clearance

[a]Calculated according to: $\sqrt{e^{\omega} - 1} \times 100\%$

Combining the IIV terms of CL_{PIP} and CL_{TAZ} reduced the AIC (ΔAIC = − 6.57) but caused an increase in the estimate for DEC_{50_TAZ} (+ 19.1 years). When the approach of covariance estimation was performed (instead of combining eta terms as in the final model) fewer pairs of IIV terms could be implemented (V_1 and V_2, but not CL or Q_2) before numerical issues occurred. The resulting model fitted the data more poorly than the final model (ΔAIC = + 95.2). Similarly, when estimating different eta magnitudes, fewer pairs of IIV terms could be implemented (V_1 and V_2, but not CL or Q_2) before numerical issues occurred and the model fitted the data more poorly than the final model (ΔAIC = 91.2).

Merging each pair of parallel residual error magnitude resulted in a significant increase of AIC (ΔAIC = + 7.39 to + 9.133), indicating that the residual-error distributions for PIP are significantly different from those for TAZ. We also considered including off-diagonal elements in $SIGMA but the complexity of the error model with proportional-additive (PIP total/DBS, and unbound) and proportional (TAZ) components made it difficult to construct a model capturing this intent.

After completing the evaluation of correlations between the PK of PIP and TAZ, we tested a model consisting of a parallel linear and non-linear elimination pathway for PIP (for details the reader is referred to ESM2 and in particular Eqs S1–S3). The inclusion of this parallel linear and non-linear elimination pathway did not improve the fit of the model to the data (ΔAIC = + 2.3).

The final combined PK model for PIP/TAZ was thereby obtained, which is shown in Table 3 and Eqs. 6–25.

$$V_{1\_PIP}(\mathrm{L}) = \theta_{V1\_PIP} \times F_{SIZE} \times e^{\eta_1}, \tag{6}$$

$$\mathrm{CL_{PIP}}\left(\mathrm{L\ h^{-1}}\right) = \theta_{CL\_PIP} \times F_{SIZE}{}^{0.75} \times F_{MAT} \times F_{DEC\_PIP} \times F_{SCR} \times \theta_{CL\_Sime} \times e^{\eta_2}, \tag{7}$$

$$V_{2\_PIP}(\mathrm{L}) = \theta_{V2\_PIP} \times F_{SIZE} \times \theta_{V2\_Sime} \times e^{\eta_4}, \tag{8}$$

$$Q_{2\_PIP}\left(\mathrm{L\ h^{-1}}\right) = \theta_{Q2\_PIP} \times \left(\frac{V_{2\_PIP}}{\theta_{V2\_PIP}}\right)^{0.75} \times e^{\eta_5}, \tag{9}$$

$$\mathrm{IPRED_{PIP}}\left(\mathrm{mg\ L^{-1}}\right) = \frac{A_{1\_PIP}}{V_{1\_PIP}} \times f_{UNB\_PIP} \times f_{DBS\_PIP}, \tag{10}$$

$$V_{1\_TAZ}(\mathrm{L}) = \theta_{V1\_TAZ} \times F_{SIZE} \times e^{\eta_1}, \tag{11}$$

$$\mathrm{CL_{TAZ}}\left(\mathrm{L\ h^{-1}}\right) = \theta_{CL\_TAZ} \times F_{SIZE}{}^{0.75} \times F_{MAT} \times F_{DEC\_TAZ} \times F_{SCR} \times e^{\eta_3}, \tag{12}$$

$$V_{2\_TAZ}(\mathrm{L}) = \theta_{V2\_TAZ} \times F_{SIZE} \times e^{\eta_4}, \tag{13}$$

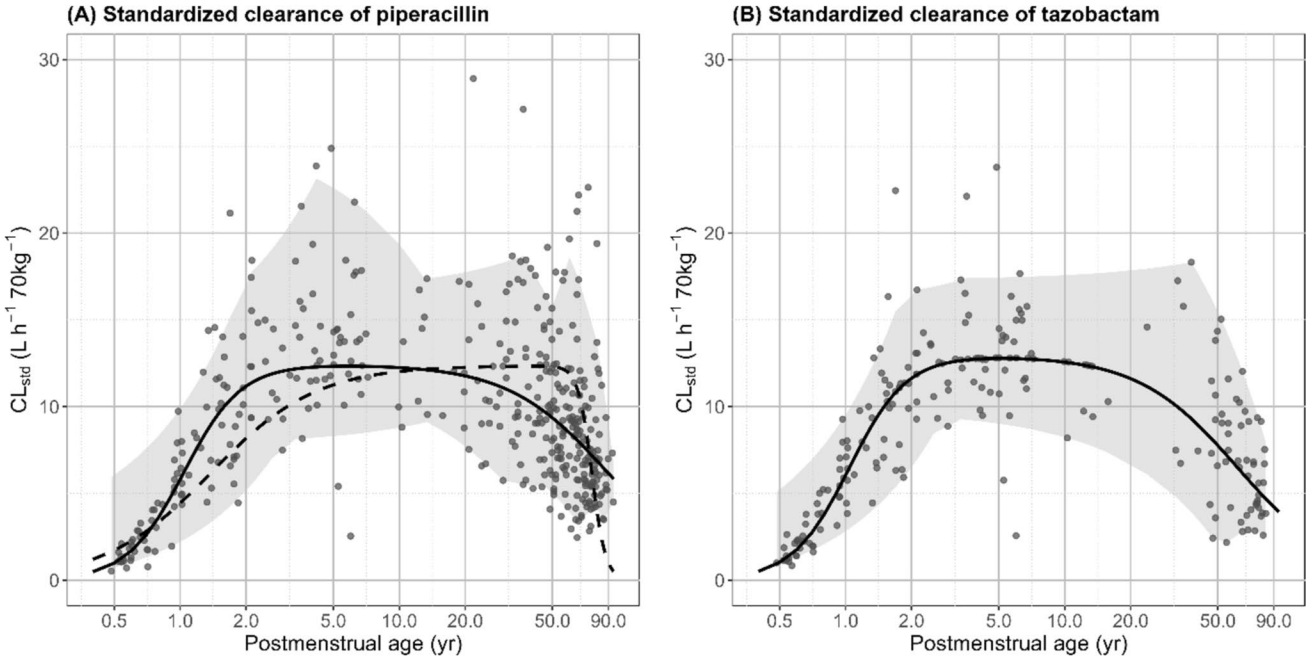

Fig. 1 Standardised clearance [CL_{std}] (L h^{-1} 70 kg^{-1}) of piperacillin (PIP, **A**) and tazobactam (TAZ, **B**) throughout life. The solid lines represent the typical CL_{std} of PIP and TAZ according to our final combined pharmacokinetic (PK) model. The solid grey circles represent the post hoc CL_{std} values for all patients included in this study. The region between the 5% and 95% percentile of those post hoc CL_{std} values is shown with grey shadow. The maturation-decline function for PIP according to the Lonsdale et al. [6] study is shown by the dashed line

$$Q_{2\_TAZ}\left(\mathrm{L\,h^{-1}}\right) = \theta_{Q2\_TAZ} \times \left(\frac{V_{2\_TAZ}}{\theta_{V2\_TAZ}}\right)^{0.75} \times e^{\eta_5}, \tag{14}$$

$$\mathrm{IPRED}_{TAZ}\left(\mathrm{mg\,L^{-1}}\right) = \frac{A_{1\_TAZ}}{V_{1\_TAZ}} \times f_{DBS\_TAZ}, \tag{15}$$

$$F_{SIZE} = \frac{\mathrm{TBW(kg)}}{70}, \tag{16}$$

$$F_{MAT} = \frac{\mathrm{PMA(week)}^{\gamma_1}}{\mathrm{PMA(week)}^{\gamma_1} + \mathrm{MAT_{50}}^{\gamma_1}}, \tag{17}$$

$$F_{DEC\_PIP} = 1 - \frac{\mathrm{PMA(year)}^{\gamma_2}}{\mathrm{PMA(year)}^{\gamma_2} + \mathrm{DEC_{50\_PIP}}^{\gamma_2}}, \tag{18}$$

$$F_{DEC\_TAZ} = 1 - \frac{\mathrm{PMA(year)}^{\gamma_2}}{\mathrm{PMA(year)}^{\gamma_2} + \mathrm{DEC_{50\_TAZ}}^{\gamma_2}}, \tag{19}$$

$$\mathrm{SCR_{std}} = \mathrm{e}^{\left[1.42 - \frac{(1.17 + 0.203 \times \ln(\mathrm{PMA(year)}/100))}{\sqrt{\mathrm{PMA(year)}/100}}\right]}, \tag{20}$$

$$\theta_{CL\_Sime} = \begin{cases} 1.73, & \textit{for the study by Sime et al.}\,[7] \\ 1, & \textit{for other included studies} \end{cases}, \tag{21}$$

$$\theta_{V2\_Sime} = \begin{cases} 0.512, & \textit{for the study by Sime et al.}\,[7] \\ 1, & \textit{for other included studies} \end{cases}, \tag{22}$$

$$f_{UNB\_PIP} = \begin{cases} 0.645, & \textit{for } C_{UNB} \textit{ observations of PIP which are not from the Sukarnjanaset et al.}\,[11] \textit{ study} \\ 1, & \textit{for other observations} \end{cases}, \tag{23}$$

Table 3 Parameter estimates and associated relative standard errors (RSEs) for the final combined population-pharmacokinetic model for piperacillin/tazobactam. Inter-individual variability (IIV) associated with the typical parameters is expressed as coefficient of variation%. Residual errors are expressed as standard deviation

Parameter	Estimate (95% CI)[a] [η or ε shrinkage,%]	
	Piperacillin	Tazobactam
θ_{V1} (L 70 kg^{-1})	10.4 (9.54, 11.2)	10.5 (9.49, 11.6)
θ_{CL} (L h^{-1} 70 kg^{-1})	10.6 (9.77, 11.2)	9.58 (8.44, 10.6)
θ_{V2} (L 70 kg^{-1})	11.6 (10.4, 12.8)	13.7 (12.4, 15.3)
θ_{Q2} (L h^{-1} 70 kg^{-1})	15.2 (12.8, 17.9)	16.8 (14.1, 20.0)
MAT_{50} (week)	54.2 (49.2, 140)	
γ_1	3.35 (2.90, 3.95)	
DEC_{50} (year)	89.1 (77.5, 109)	61.6 (50.0, 72.0)
γ_2	1.92 (1.27, 2.68)	
θ_{SCR} (dL mg^{-1})	0.346 (0.321, 0.375)	
f_{UNB}	0.645 (0.606, 0.689)	–
$f_{UNB\_Sukarnjanaset}$	1 FIX	–
f_{DBS}	0.368 (0.338, 0.398)	0.448 (0.419, 0.478)
θ_{CL_Sime}	1.73 (1.41, 2.16)	–
θ_{V2_Sime}	0.512 (0.299, 0.846)	–
IIV of V_1 (%)[b]	42.6 (36.4, 48.9) [41.0]	
IIV of CL (%)[b]	43.2 (40.0, 47.0) [7.0]	41.5 (37.6, 45.8) [37.1]
IIV of V_2 (%)[b]	85.4 (73.4, 99.5) [21.0]	
IIV of Q_2 (%)[b]	65.6 (52.7, 84.0) [44.6]	
$\sigma_{TOT\&DBS}$ (proportional) (%)[c]	30.2 (29.2, 31.1) [8]	28.5 (27.5, 29.5) [6]
$\sigma_{TOT\&DBS}$ (additive) (mg L^{-1})[c]	0.147 (0.0827, 0.199) [8]	0 FIX [100]
σ_{UNB} (proportional) (%)[c]	36.5 (34.1, 38.6) [10]	–
σ_{UNB} (additive) (mg L^{-1})[c]	0.747 (0.361, 1.07) [10]	–

CI confidence interval, *CL* elimination clearance, DEC_{50} the postmenstrual age when elimination clearance decreases to 50% of the maximum value, f_{DBS} ratio of total drug concentration in dried blood spot samples to those in plasma samples, f_{UNB} fraction unbound in studies except the one by Sukarnjanaset et al. [11], $f_{UNB\_Sukarnjanaset}$ fraction unbound in the Sukarnjanaset et al. [11] study, *IIV* inter-individual variability, MAT_{50} the postmenstrual age when elimination clearance increases to 50% of the maximum value, Q_2 inter-compartment clearance, V_1 central volume of distribution, V_2 peripheral volume of distribution, γ_1 shape factor for maturation of CL, γ_2 shape factor for decline of CL, θ_{CL_Sime} relative elimination clearance for piperacillin in the study of Sime et al. [7] which in which subjects were patients with haematological malignancies, θ_{SCR} effect coefficient of serum creatinine on elimination clearance, θ_{V2_Sime} relative volume of distribution for peripheral compartment for piperacillin in the study of Sime et al. [7], $\sigma_{TOT\&DBS}$ residual error for total drug concentration in plasma samples and dried blood samples, σ_{UNB} residual error for unbound plasma concentration

[a]Derived from results of sampling importance resampling [39]

[b]Calculated according to: $\sqrt{e^{\omega}-1}\times 100\%$

[c]Proportional residual errors were calculated according to: $\sqrt{\sigma}\times 100\%$, additive residual errors were calculated according to: $\sqrt{\sigma}$

$$f_{\mathrm{DBS\_PIP}} = \begin{cases} 0.368, & \textit{for } C_{\mathrm{DBS}} \textit{ observations of PIP} \\ 1, & \textit{for other observations} \end{cases}, \quad (24)$$

$$f_{\mathrm{DBS\_TAZ}} = \begin{cases} 0.448, & \textit{for } C_{\mathrm{DBS}} \textit{ observations of TAZ} \\ 1, & \textit{for other observations} \end{cases}, \quad (25)$$

In above equations, the parameters with subscript PIP are only used to describe the PK of piperacillin while those with subscript TAZ are exclusively used to describe the PK of tazobactam. V_1 and V_2 are the central and peripheral volume of distribution; CL and Q_2 denote the elimination and inter-compartment clearance. Size-related changes, PMA-induced maturation, PMA-induced decline, and SCR-related changes in the PK of PIP/TAZ are described by F_{SIZE}, F_{MAT}, F_{DEC} and F_{SCR}, respectively. The $\theta_{\mathrm{CL\_Sime}}$ and $\theta_{\mathrm{V2\_Sime}}$ represent the elevated $\mathrm{CL_{PIP}}$ and decreased $\mathrm{V_{2\_PIP}}$ in patients with haematological malignancies [7]. η_i (i = 1–5), with variances of ω_i, represent IIV of typical PK parameters. The f_{UNB} and the f_{DBS} are the fraction unbound and the ratio of C_{DBS} to C_{TOT}. IPRED represent individual predictions of all kinds of

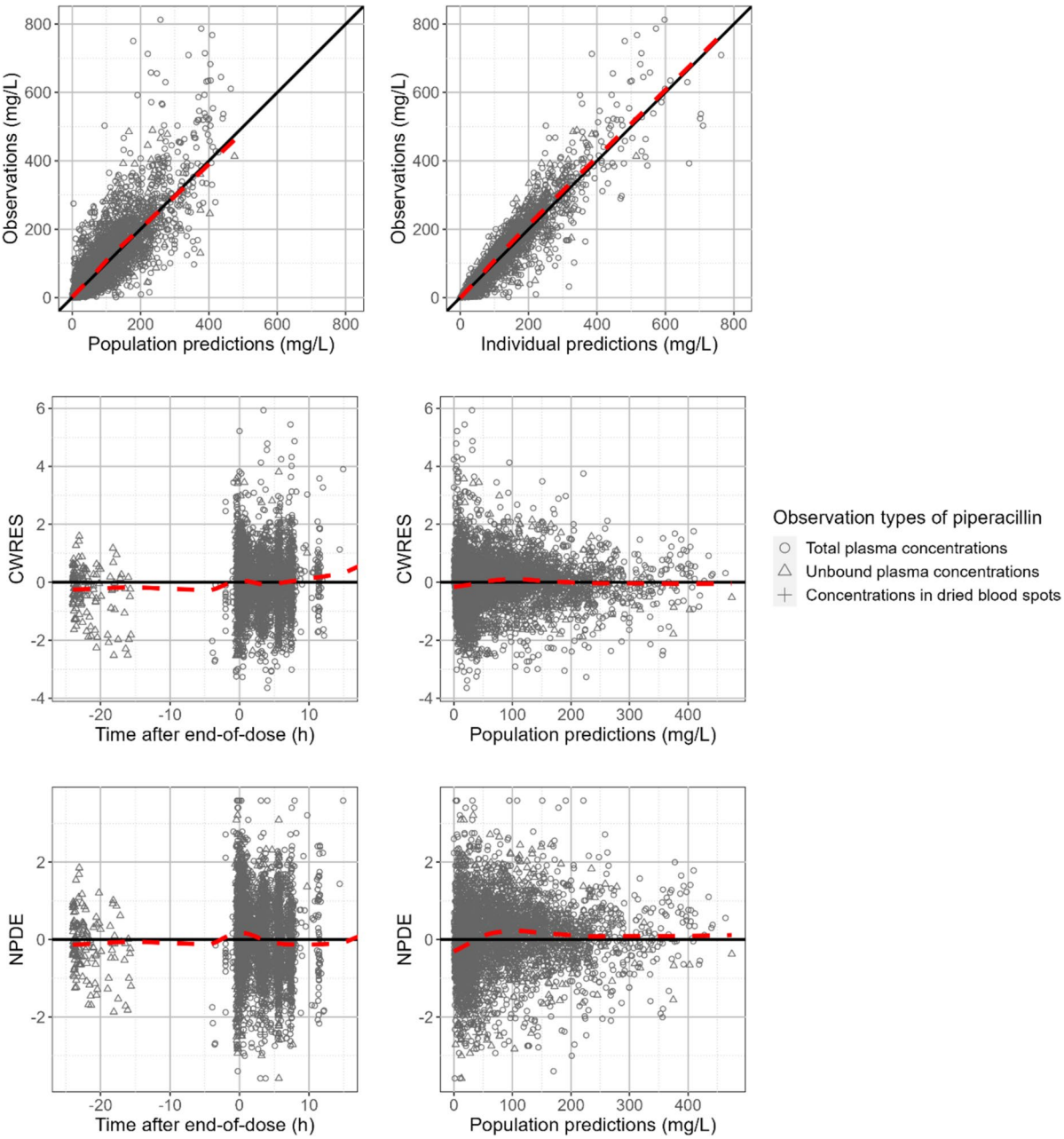

Fig. 2 Goodness-of-fit plots for the final combined population pharmacokinetic model for piperacillin concentrations. Scatterplots show the distributions of observed piperacillin concentrations versus population and individual predictions, conditionally weighted residuals (CWRES) versus population predictions and time after the end of the dose, as well as normalised prediction distribution errors (NPDE) versus population predictions and time after the end of the dose. Circles, triangles and crosses denote total plasma concentrations, unbound plasma concentrations, and concentrations in dried blood spots, respectively. Solid black lines represent lines of unity or zero lines. Red dashed lines are non-parametric smoothers of those distributions. Negative time points mean that observations were collected during the infusion, while positive time points denote observations taken after the infusion is finished

observations. A_1 denotes predicted amounts in the central compartments.

Backwards elimination of F_{SIZE}, F_{MAT}, F_{DEC} or F_{SCR} led to significant OFV increases and difficulties in convergences. Goodness-of-fit and pvcVPC plots for the final combined PK model for PIP/TAZ are shown in Figs. 2, 3, 4. In addition, Figures S3–S4 in the ESM1 show the GOF and pvcVPC plots stratified by observation type and patient subgroup. Our combined model shows acceptable performance across these diagnostics, despite the apparent underprediction of PIP in the first 1–2 hours after stopping the infusion (Fig. 4). The underprediction

does not seem to be specific to any subgroup (Fig. S4). We were unable to remove this underprediction in model development. Model code of the final PIP/TAZ population PK model is available in ESM3.

3.4 Evaluation of Current Dosing Recommendations

Simulated dosing regimens and characteristics of the virtual patients were summarised in Table S3 of the ESM4. The SmPC label does not provide specific dosing recommendations for neonates and infants. In the simulations for the SmPC dosing recommendations, the lowest weight-based dose from the SmPC label (70/8.75 mg kg^{-1} PIP/TAZ every 8 h) was applied for both age groups. Similarly, the lowest weight-based dose from the FDA label (80/10 mg kg^{-1} PIP/TAZ every 8 h) was used for neonates in the simulations for the FDA dosing recommendations.

The simulated steady-state PTA versus MIC profiles resulting from the dosing recommendations in the SmPC label are shown in Fig. 5.

Simulations for both the SmPC (Fig. 5) and the FDA dosing recommendations (Fig. S5) show that PTA versus MIC profiles are considerably different across age groups, suggesting that current dosing recommendations do not result in consistent PTAs across age groups. The highest PTAs are found in neonates and the lowest in infants, even though dosing recommendations for these groups are weight adjusted. A similar but smaller difference is apparent between elderly and adults, as well as adolescents and children, with PTAs being higher in elderly compared to adults and higher in adolescents compared to children.

The PTA versus MIC profiles of the SmPC dosing recommendations (Fig. 5) and the FDA dosing recommendations (Fig. S5) shift to the right for longer duration infusions indicating higher PTAs are obtained. The PTAs are highest and have lowest variability for continuous infusions, indicating that most patients receive an effective treatment.

In addition, C_{m_TAZ} was calculated across different age groups to evaluate the steady-state TAZ exposure achieved by the recommended dosing regimens. The median unbound TAZ concentration (considering $f_{UNB\_TAZ} = 70\%$ [49]) across age groups and simulated scenarios was 3.69 mg L^{-1} (ranging from 1.64 to 6.77 mg L^{-1}), with the lowest exposure occurring in the infants.

4 Discussion

In this pooled population PK analysis, we described how the PK of PIP/TAZ changes throughout life using a 4-compartment combined population PK model in which V_{1_PIP}, V_{2_PIP}, V_{1_TAZ}, and V_{2_TAZ} were estimated as 0.149 L kg^{-1}, 0.166 L kg^{-1}, 0.150 L kg^{-1}, and 0.196 L kg^{-1}, respectively. Those results differ from the Hemmersbach-Miller et al. [4] study in which the PK of PIP and TAZ in adults were characterised by 1-compartment models with considerably different V_{1_PIP} (0.357 L kg^{-1}) and V_{1_TAZ} (0.453 L kg^{-1}). According to our final combined model, typical CL_{PIP} and CL_{TAZ} for a 30-year-old, 70-kg adult with a SCR of 0.773 mg dL^{-1} and a CL_{CR} of 131 mL min^{-1} are 11.0 L h^{-1} and 10.3 L h^{-1}, respectively. For a 70-year-old, 70-kg patient with a SCR of 1.12 mg dL^{-1} and a CL_{CR} of 68.4 mL min^{-1}, CL_{PIP} and the CL_{TAZ} are 7.33 L h^{-1} and 5.37 L h^{-1}, respectively. These estimates are close to those predicted by the Hemmersbach-Miller et al. [4] model (CL_{PIP} = 10.2 L h^{-1}, CL_{TAZ} = 10.8 L h^{-1} for a 30-year-old patient; CL_{PIP} = 6.49 L h^{-1}, CL_{TAZ} = 6.13 L h^{-1} for a 70-year-old patient). For a 44.3-week PMA (40 weeks gestational age + 1 month PNA), a 4.5-kg infant with a SCR of 0.416 mg dL^{-1}, typical CL_{PIP} is estimated as 0.543 L h^{-1} in our model, which is relatively larger than the value reported by Barker et al. [50] (0.424 L h^{-1}) but lower than the estimate in the Li et al. [51] model (1.15 L h^{-1}). Also, the typical CL_{TAZ} for this child is predicted to be 1.41 L h^{-1} based on the model of the Li et al. [51] and is much higher than our estimate (0.565 L h^{-1}). Sime et al. [7] reported an elevated volume of distribution in haematological malignancy patients compared to other patient populations. In contrast, we found a lower V_2 (− 48.8%) for haematological malignancy patients using the same data as a part of a pooled analysis. The benefit of a pooled model is that it allows to identify the specific parameters that differ in this subgroup of patients.

According to our final combined PK model, MAT_{50_PIP} and DEC_{50_PIP} are 54.2 weeks and 89.1 years PMA, respectively, which is in line with the estimates (MAT_{50_PIP} = 71.6 weeks PMA (95% confidence interval [CI] 39.3–104), DEC_{50_PIP} = 75.6 years PMA (95% CI 36.0–115) in the pooled analysis of Lonsdale et al. [6]. We found that CL_{TAZ} has the same maturation process as CL_{PIP}; however, CL_{TAZ} declines faster. Considering that the organic anion transporters 1/3 (OAT1/3) are the common transporters for PIP and TAZ in proximal tubular basolateral membranes with PIP having a stronger affinity than tazobactam [52], asynchrony of the two decline processes suggests that glomerular filtration declines faster than tubular secretion. As for maturation of CL, it progresses so fast that the difference between MAT_{50_PIP} and MAT_{50_TAZ} is negligible.

We found that CL_{PIP} and CL_{TAZ} are equally influenced by SCR. This is not surprising because the elimination of SCR reflects both glomerular filtration as well as tubular secretion and SCR shares the common tubular transporters with PIP and TAZ [53, 54]. Sime et al. [7] reported an elevated CL_{PIP} in the haematological malignancy patients and explained it by the augmented renal clearance. Nevertheless, we observed an extra rise of 73.2% in the CL_{PIP} in

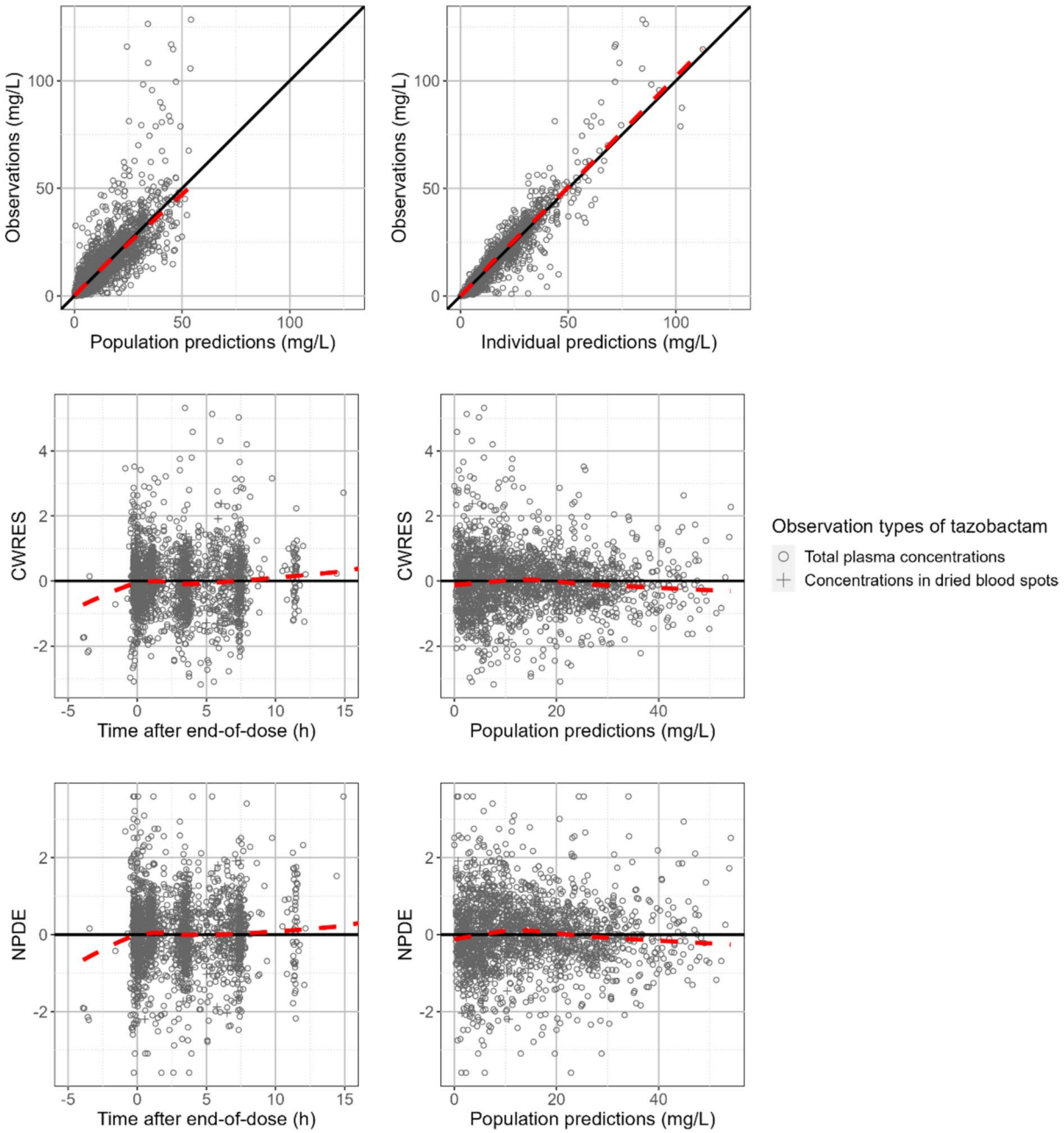

Fig. 3 Goodness-of-fit plots for the final combined population pharmacokinetic model for tazobactam concentrations. Scatterplots show the distributions of observed tazobactam concentrations versus population and individual predictions, conditionally weighted residuals (CWRES) versus population predictions and time after the end of the dose, as well as normalised prediction distribution errors (NPDE) versus population predictions and time after the end of the dose. Circles and crosses denote total plasma concentrations and concentrations in dried blood spots, respectively. Solid black lines represent lines of unity or zero lines. Red dashed lines are non-parametric smoothers of those distributions. Concentrations with negative times were collected during the infusion, while positive times denote observations taken after the infusion was finished

those patients after we corrected the PK of PIP for SCR-related changes, which indicates that there are additional factors contributing to the CL_{PIP} increase in haematological malignancy patients.

Previous studies have shown that CL_{PIP} is saturable [3, 5, 32]. To test this hypothesis, we explored models assuming (1) a single saturable elimination pathway and (2) a parallel linear and non-linear elimination pathway. Neither led to a significant improvement in GOF. Although the data of Bulitta et al. [5] and Landersdorfer et al. [3] were not part of this pooled analysis, and may present a unique subgroup of patients, our analysis suggests that CL_{PIP} is not saturable

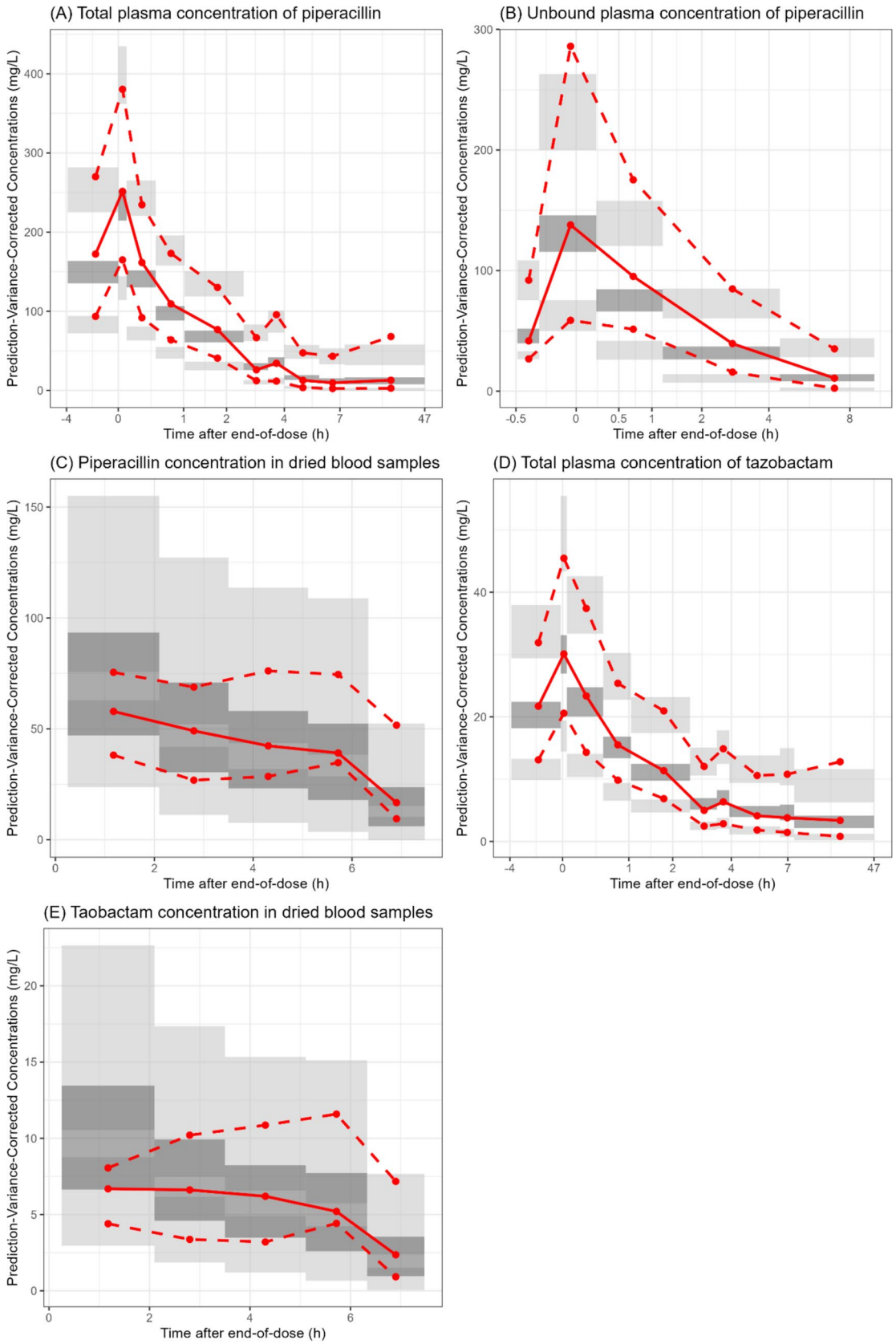
(A) Total plasma concentration of piperacillin
Prediction-Variance-Corrected Concentrations (mg/L)
Time after end-of-dose (h)
(B) Unbound plasma concentration of piperacillin
Prediction-Variance-Corrected Concentrations (mg/L)
Time after end-of-dose (h)
(C) Piperacillin concentration in dried blood samples
Prediction-Variance-Corrected Concentrations (mg/L)
Time after end-of-dose (h)
(D) Total plasma concentration of tazobactam
Prediction-Variance-Corrected Concentrations (mg/L)
Time after end-of-dose (h)
(E) Taobactam concentration in dried blood samples
Prediction-Variance-Corrected Concentrations (mg/L)
Time after end-of-dose (h)

◂**Fig. 4** Prediction- and variability-corrected visual predictive check plots for the final combined population pharmacokinetic model for total plasma concentrations of piperacillin (**A**), unbound plasma concentrations of piperacillin (**B**), piperacillin concentrations in dried blood spots (**C**), total plasma concentrations of tazobactam (**D**) and tazobactam concentrations in dried blood spots (**E**), respectively. Solid red lines are the 50th percentiles of observations corrected by prediction and variance, while dashed red lines denote the 10th and 90th percentiles. Red dashed lines are non-parametric smoothers of those distributions. Negative time points mean that observations were collected during the infusion, while positive time points denote observations taken after the infusion is finished. Grey shaded rectangles represent the 95% confidence intervals for the simulated 10th, 50th and 90th percentiles of the prediction- and variance-corrected observations

within the range of clinically relevant PIP concentrations that were included in this study. A single non-linear elimination pathway for TAZ did not improve overall model fit. Therefore, we concluded that saturable clearance of TAZ is not supported by our data.

In our final combined PK model, the f_{UNB_PIP} was estimated as 64.5%, relatively lower than the previous reported values [21, 22]. Considering that only 20 patients had both C_{TOT} and C_{UNB} observations of PIP, more data are needed to quantify the population variability in f_{UNB_PIP} and its dependence on patient/trial characteristics. Only two studies provided both C_{UNB} of PIP and serum albumin concentrations, which we considered too few to consider albumin concentrations in model development. We also tested non-linear protein binding of PIP but found that it did not improve the model. Other non-linear dynamics (e.g., non-linear distribution models) were not considered in our study.

In addition, the f_{DBS_PIP} and the f_{DBS_TAZ} for infants from the Cohen-Wolkowiez et al. [8] study were estimated as 36.8% and 44.8% in this pooled analysis, respectively. These estimates are in agreement with the values (f_{DBS_PIP} = 38%, f_{DBS_TAZ} = 48%) that Cohen-Wolkowiez et al. [8] obtained in their compartmental models.

We found that using one parameter to simultaneously characterise the IIV of Q_{2_PIP} and Q_{2_TAZ} led to better goodness of fit without disturbing the estimation of the fixed-effect parameters in combined models. Such a correlation was addressed in each pair of parallel IIV terms on volume terms (V_{1_PIP}, V_{1_TAZ}, V_{2_PIP}, V_{2_TAZ}). This result is consistent with the earlier work of Wallenburg et al. [49] and suggests that if a patient has a relatively higher/lower volume of distribution of PIP, then his/her volume of distribution of TAZ is equally higher/lower than the typical value. However, we failed to identify the correlation between IIV of CL_{PIP} and CL_{TAZ}. More data are needed to analyse this correlation, whereas common IIV parameter and covariance both result in significant OFV decrease.

The model's underprediction of PIP concentrations in the first 1–2 h after stopping the infusion (as seen in Fig. 4) is unlikely to have a meaningful clinical impact. First, Fig. 4 suggests that the underprediction is transient. Second, dose adjustments are typically recommended based on PIP samples taken at steady-state or close to trough concentration time points where the influence of this underprediction will likely have attenuated. Third, the influence of the underprediction on dosing recommendations will result in higher doses being recommended (e.g., in MIPD tools) and consequently an overshoot of the target concentration, which in light of the safety profile of PIP is less of a concern compared to under dosing. Nonetheless, a clinical validation study should be conducted before implementing our model in clinical practice (e.g., in MIPD tools) to guarantee adequate model performance.

Monte Carlo simulations using the final combined model were performed to evaluate the PIP/TAZ dosing regimens recommended by the SmPC and the FDA label. Considerable PTA differences across different age groups were observed. Some of those discrepancies seem to be a result of not accounting for the maturation-decline function for CL_{PIP}. For instance, neonates are predicted to have higher PTAs than infants despite receiving the same dose per kg. This can be explained by maturation of CL_{PIP} in early life, resulting in a higher typical CL_{PIP} per kg for the infants compared to neonates (0.235 L h^{-1} kg^{-1} vs 0.0648 L h^{-1} kg^{-1}). Similarly, the lower typical CL_{PIP} per kg in elderly compared to adult patients (0.102 L h^{-1} kg^{-1} vs 0.132 L h^{-1} kg^{-1}) results in a higher PTA in elderly when the same dose per kg is applied. Another cause of the PTA discrepancies across different age groups is the mismatch between allometric theory and the current dosing recommendations. According to the theory-based allometric scaling [33], the CL per kg decreases with increasing weight. With greater TBW, adolescents are predicted to have a lower CL_{PIP} per kg than children (0.203 L h^{-1} kg^{-1} vs 0.253 L h^{-1} kg^{-1}) while there is full maturation and a negligible decline of CL_{PIP} in both age groups. This leads to higher predicted PTAs for adolescents compared to children in the simulations for the FDA label where both groups receive the same dosing regimen (Fig. S5). It may be advantageous to adjust the current PIP/TAZ dosing recommendations based on allometric theory and the maturation-decline function for CL_{PIP}, to obtain more consistent target attainment across age groups.

Moreover, our simulation results indicated that prolonging the duration of infusion enhances attainment of $fT_{>MIC}$ 100% and $fT_{>4*MIC}$ 100% at steady state for all age groups under the recommended dosing regimens. This is in line with previous studies [4, 55]. This can be explained by the fact that a longer infusion duration leads to a higher

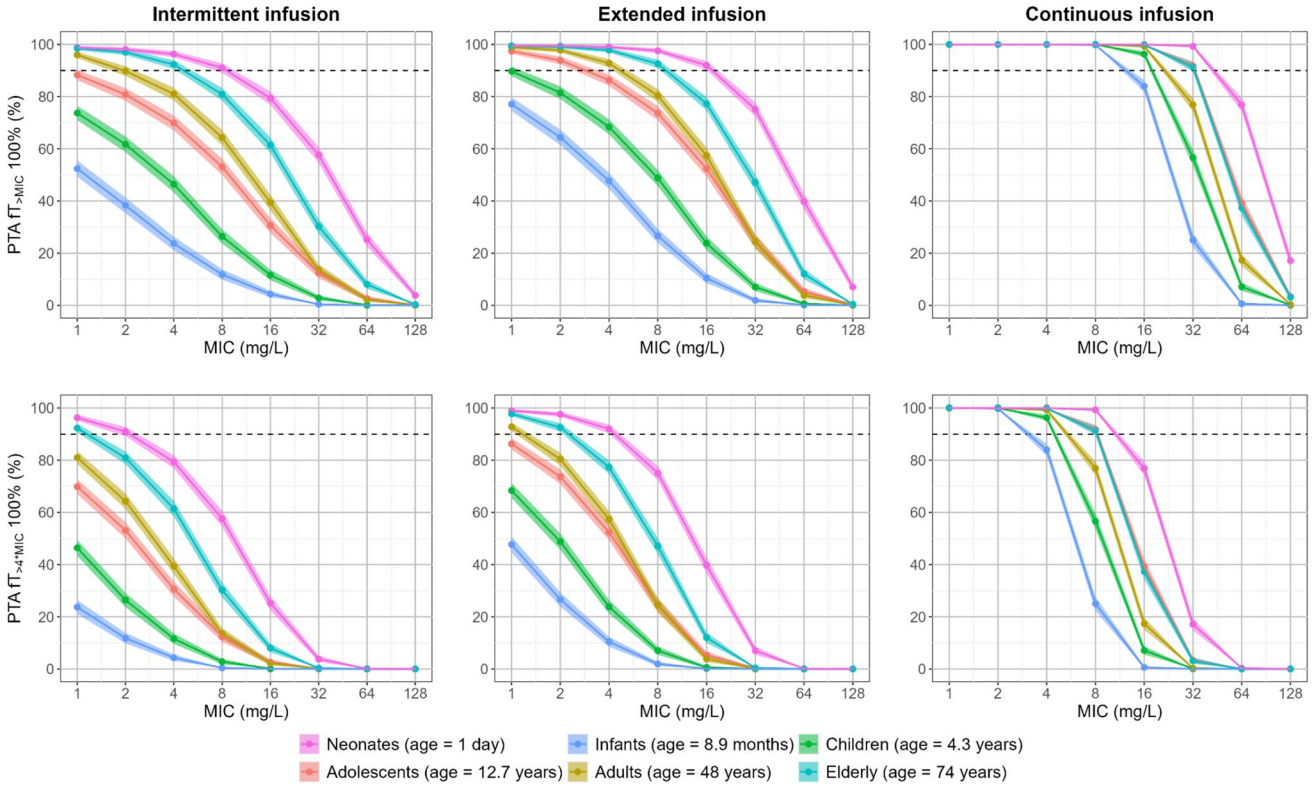

Fig. 5 Simulated probability of target attainment (PTA) of piperacillin (PIP) at steady state for different age groups of virtual patients with the highest dose according to the summary of product characteristics (SmPC) label. The PTAs of the target that unbound plasma concentration of PIP remain above the minimum inhibitory concentration (MIC) for the whole dosing interval (PTA $fT_{>MIC}$ 100%) and the PTAs of the target that the unbound plasma concentration of PIP remain above four times the MIC for the whole dosing interval (PTA $fT_{>4*MIC}$ 100%) are shown in the top and the bottom rows, respectively. PTAs under intermittent, extended, and continuous infusion are shown in the left, the middle and the right columns, respectively. PTA for different age groups are shown in different colors. The shadow areas represent the 95% confidence intervals of the PTA versus MIC curves. The dashed lines denote the PTA of 90%

steady-state trough concentration when patients receive the same dose. Our simulations also show that PTA differences between age groups are attenuated when the infusion durations are extended from intermittent infusions to extended and continuous infusions, which indicates that patients with higher CL_{PIP} per kg benefit more from the extension of infusion duration.

In addition to a high PTA of PIP, TAZ exposure should be high enough to ensure adequate beta-lactamase inhibition. As shown by Assefa et al. [56], at the moment it is difficult to draw inference on the optimum index and associated target exposure for beta-lactamase inhibitors. At the same time, beta-lactam MICs depend on high enough exposure of the co-administered beta-lactamase inhibitor [57]. To place our results in context with the work by Assefa et al. [56], Bentley [57], and future work on this topic, we reported the TAZ exposure across different age groups and simulated scenarios. We found that for infants the PTA of PIP was lower compared to the other age groups and, consequently, also the TAZ exposure was lower. Despite the uncertainty around the optimal PK/PD targets and beta-lactamase inhibitor target concentrations, our results suggest that infants may benefit from higher PIP/TAZ dosing regimens than those that are currently recommended.

There are limitations to our work. First, patients receiving renal replacement therapy or extra-corporeal membrane oxygenation were excluded from our study. Second, underweight adults (aged > 18 years and body mass index < 18.5 kg m^{-2}) were sparsely populated in our pooled dataset and therefore the performance of our model in these populations is less certain. Third, there were only three studies contributing C_{UNB} observations. One of these studies appeared to be an outlier, with a f_{UNB_PIP} higher than expected (100%) [11], forcing us to handle that study differently in this analysis. Fourth, the PTA of TAZ is not considered due to the current uncertainty on optimum TAZ target exposures. Nevertheless, our model could be used to guide optimum dosing based on combined PTA of PIP and TAZ once such information becomes available in the future. Finally, it was reported that co-administration of PIP could increase the area under the curve (AUC) of TAZ by reducing the renal excretion [22, 58,

59]. Due to the lack of TAZ monotherapy data, we were not able to confirm or negate this hypothesis.

5 Conclusion

In this study, we established a combined population PK model which is generalisable for PK changes of PIP/TAZ throughout human life. This model can be used as a robust a priori model for Bayesian forecasting to achieve individualised dosing based on TDM an lower the risk of a mismatch between the patient population and the a priori PK model. Through simulations, we showed that there are considerable differences in the steady-state PTAs across age groups under current recommended dosing regimens and adjustments based on the allometric theory and the maturation-decline function for CL_{PIP} may help to achieve more consistent target attainment.

Supplementary Information The online version contains supplementary material available at https://doi.org/10.1007/s40262-024-01460-6.

Acknowledgements Collaborators (Piperacillin/Tazobactam [PIP/TAZ] Consortium): Caroline Damen[1], Evelyn Dhont[1,2], Charlotte Kloft[3], Michael Zoller[4], Johannes Zander[5], Aziz Alobaid[6]; [1]Department of Basic and Applied Medical Sciences, Ghent University, De Pintelaan 185, 9000 Ghent, Belgium; [2]Department of Paediatric Intensive Care, Ghent University Hospital, De Pintelaan 185, 9000 Ghent, Belgium; [3]Dept. of Clinical Pharmacy & Biochemistry, Institute of Pharmacy, Freie Universität Berlin, Germany; [4]Department of Anesthesiology, University Hospital, Ludwig Maximilians University of Munich, Munich, Germany; [5]Institute of Laboratory Medicine, Hospital of the Ludwig-Maximilians-University of Munich, Munich, Germany; [6]University of Queensland Centre for Clinical Research, Faculty of Medicine, University of Queensland, Herston, Brisbane, Queensland, Australia.

Declarations

Funding This study was supported by departmental funding and China Scholarship Council to Daming Kong (202006010035).

Conflict of interest Daming Kong, Jeffrey Lipman, Fabio Silvio Taccone, Michael Cohen-Wolkowiez, Fekade B. Sime, Danny Tsai, Pieter A. J. G. De Cock, Sutep Jaruratanasirikul, Sofie A. M. Dhaese, Andrew A. Udy, Robin Michelet, Céline Thibault, Jeroen V. Koomen, Douglas J. Eleveld, Michel M. R. F. Struys, Evelyn Dhont, Caroline Damen, Charlotte Kloft, Michael Zoller, Johannes Zander and Aziz Alobaid certify that they have no affiliations with or involvement in any organisation or entity with any financial interest or non-financial interest in the subject matter or materials discussed in this manuscript. Over the last 3years Pieter J. Colin and his research group has been involved in contract research for PAION UK Ltd. (London, England) and Acacia Pharma Ltd. (Cambridge, England). Jason A. Roberts has received funding from the Australian National Health and Medical Research Council for a Centre of Research Excellence (APP2007007) and an Investigator Grant (APP2009736) as well as an Advancing Queensland Clinical Fellowship. Timothy W. Felton is supported by the NIHR Manchester Biomedical Research Centre (NIHR203308). Jan J. De Waele is supported by a Sr Clinical Research Grant from the Research Foundation Flanders (FWO, Ref. 1881020N). He has consulted for Menarini, MSD, Pfizer, ThermoFisher and Viatris (fees and honoraria paid to institution).

Authors' contributions Daming Kong, Pieter J. Colin, Douglas J. Eleveld and Jeroen V. Koomen contributed to the study conception and design. Data collection was performed by Jason A. Roberts, Jeffrey Lipman, Fabio Silvio Taccone, Michael Cohen-Wolkowiez, Fekade B. Sime, Danny Tsai, Pieter A. J. G. De Cock, Sutep Jaruratanasirikul, Sofie A. M. Dhaese, Andrew A. Udy, Timothy W. Felton, Robin Michelet, Céline Thibault, Julie Autmizguine and Pieter J. Colin. Data analysis was performed by Daming Kong. The first draft of the manuscript was written by Daming Kong and all authors reviewed and edited previous versions of the manuscript. All authors read and approved the final manuscript.

Collaborators' contributions Caroline Damen contributed to the literature search. Charlotte Kloft, Michael Zoller and Johannes Zander contributed to the planning and execution of some of the studies underlying the dataset. All collaborators contributed to collection and preprocessing of the data.

Data availability Data will be made available upon reasonable request to the corresponding author and only if the authors of the original clinical trial agree with the transfer of the data.

Ethics approval Institutional review board approval was attained for all original studies included in our analysis.

Consent to participate Not applicable.

Consent for publication Not applicable.

Code availability The NONMEM code for the final PIP/TAZ population PK model is available in ESM3.

References

1. El-Haffaf I, Caissy JA, Marsot A. Piperacillin-tazobactam in intensive care units: a review of population pharmacokinetic analyses. Clin Pharmacokinet. 2021;60(7):855–75. https://doi.org/10.1007/s40262-021-01013-1.
2. Hayashi Y, et al. Pharmacokinetic evaluation of piperacillin-tazobactam. Expert Opin Drug Metab Toxicol. 2010;6(8):1017–31. https://doi.org/10.1517/17425255.2010.506187.
3. Landersdorfer CB, et al. Population pharmacokinetics of piperacillin at two dose levels: influence of nonlinear pharmacokinetics

on the pharmacodynamic profile. Antimicrob Agents Chemother. 2012;56(11):5715–23. https://doi.org/10.1128/AAC.00937-12.
4. Hemmersbach-Miller M, et al. Population pharmacokinetics of piperacillin/tazobactam across the adult lifespan. Clin Pharmacokinet. 2023;62(1):127–39. https://doi.org/10.1007/s40262-022-01198-z.
5. Bulitta JB, et al. Nonlinear pharmacokinetics of piperacillin in healthy volunteers–implications for optimal dosage regimens. Br J Clin Pharmacol. 2010;70(5):682–93. https://doi.org/10.1111/j.1365-2125.2010.03750.x.
6. Lonsdale DO, et al. Scaling beta-lactam antimicrobial pharmacokinetics from early life to old age. Br J Clin Pharmacol. 2019;85(2):316–46. https://doi.org/10.1111/bcp.13756.
7. Sime FB, et al. Altered pharmacokinetics of piperacillin in febrile neutropenic patients with hematological malignancy. Antimicrob Agents Chemother. 2014;58(6):3533–7. https://doi.org/10.1128/AAC.02340-14.
8. Cohen-Wolkowiez M, et al. Developmental pharmacokinetics of piperacillin and tazobactam using plasma and dried blood spots from infants. Antimicrob Agents Chemother. 2014;58(5):2856–65. https://doi.org/10.1128/AAC.02139-13.
9. De Cock P, et al. Dose optimization of piperacillin/tazobactam in critically ill children. J Antimicrob Chemother. 2017;72(7):2002–11. https://doi.org/10.1093/jac/dkx093.
10. Obrink-Hansen K, et al. Population pharmacokinetics of piperacillin in the early phase of septic shock: does standard dosing result in therapeutic plasma concentrations? Antimicrob Agents Chemother. 2015;59(11):7018–26. https://doi.org/10.1128/AAC.01347-15.
11. Sukarnjanaset W, Jaruratanasirikul S, Wattanavijitkul T. Population pharmacokinetics and pharmacodynamics of piperacillin in critically ill patients during the early phase of sepsis. J Pharmacokinet Pharmacodyn. 2019;46(3):251–61. https://doi.org/10.1007/s10928-019-09633-8.
12. Thibault C, et al. Population pharmacokinetics and safety of piperacillin-tazobactam extended infusions in infants and children. Antimicrob Agents Chemother. 2019. https://doi.org/10.1128/AAC.01260-19.
13. Udy AA, et al. Are standard doses of piperacillin sufficient for critically ill patients with augmented creatinine clearance? Crit Care. 2015;19(1):28. https://doi.org/10.1186/s13054-015-0750-y.
14. Alobaid AS, et al. Population pharmacokinetics of piperacillin in nonobese, obese, and morbidly obese critically ill patients. Antimicrob Agents Chemother. 2017. https://doi.org/10.1128/AAC.01276-16.
15. Roberts JA, et al. First-dose and steady-state population pharmacokinetics and pharmacodynamics of piperacillin by continuous or intermittent dosing in critically ill patients with sepsis. Int J Antimicrob Agents. 2010;35(2):156–63. https://doi.org/10.1016/j.ijantimicag.2009.10.008.
16. Tamme K, et al. Pharmacokinetics and pharmacodynamics of piperacillin/tazobactam during high volume haemodiafiltration in patients with septic shock. Acta Anaesthesiol Scand. 2016;60(2):230–40. https://doi.org/10.1111/aas.12629.
17. Vinks AA, et al. Population pharmacokinetic analysis of nonlinear behavior of piperacillin during intermittent or continuous infusion in patients with cystic fibrosis. Antimicrob Agents Chemother. 2003;47(2):541–7. https://doi.org/10.1128/AAC.47.2.541-547.2003.
18. Kalaria SN, Gopalakrishnan M, Heil EL. A population pharmacokinetics and pharmacodynamic approach to optimize tazobactam activity in critically ill patients. Antimicrob Agents Chemother. 2020. https://doi.org/10.1128/AAC.02093-19.
19. Kim YK, et al. Population pharmacokinetics of piperacillin/tazobactam in critically ill Korean patients and the effects of extracorporeal membrane oxygenation. J Antimicrob Chemother. 2022;77(5):1353–64. https://doi.org/10.1093/jac/dkac059.
20. Zhang Z, et al. Population pharmacokinetic analysis for plasma and epithelial lining fluid ceftolozane/tazobactam concentrations in patients with ventilated nosocomial pneumonia. J Clin Pharmacol. 2021;61(2):254–68. https://doi.org/10.1002/jcph.1733.
21. Martinkova J, et al. A pilot study on pharmacokinetic/pharmacodynamic target attainment in critically ill patients receiving piperacillin/tazobactam. Anaesthesiol Intensive Ther. 2016;48(1):23–8. https://doi.org/10.5603/AIT.a2015.0082.
22. Sorgel F, Kinzig M. The chemistry, pharmacokinetics and tissue distribution of piperacillin/tazobactam. J Antimicrob Chemother. 1993;31(Suppl A):39–60. https://doi.org/10.1093/jac/31.suppl_a.39.
23. Mouton JW, et al. Standardization of pharmacokinetic/pharmacodynamic (PK/PD) terminology for anti-infective drugs: an update. J Antimicrob Chemother. 2005;55(5):601–7. https://doi.org/10.1093/jac/dki079.
24. Vogelman B, et al. Correlation of antimicrobial pharmacokinetic parameters with therapeutic efficacy in an animal model. J Infect Dis. 1988;158(4):831–47. https://doi.org/10.1093/infdis/158.4.831.
25. De Waele JJ, et al. Therapeutic drug monitoring-based dose optimisation of piperacillin and meropenem: a randomised controlled trial. Intensive Care Med. 2014;40(3):380–7. https://doi.org/10.1007/s00134-013-3187-2.
26. Hagel S, et al. Effect of therapeutic drug monitoring-based dose optimization of piperacillin/tazobactam on sepsis-related organ dysfunction in patients with sepsis: a randomized controlled trial. Intensive Care Med. 2022;48(3):311–21. https://doi.org/10.1007/s00134-021-06609-6.
27. Richter DC, et al. Therapeutic drug monitoring-guided continuous infusion of piperacillin/tazobactam significantly improves pharmacokinetic target attainment in critically ill patients: a retrospective analysis of four years of clinical experience. Infection. 2019;47(6):1001–11. https://doi.org/10.1007/s15010-019-01352-z.
28. Van Wynsberge G, et al. Impact of model-informed precision dosing in adults receiving vancomycin via continuous infusion: a randomized, controlled clinical trial. Trials. 2024;25(1):126. https://doi.org/10.1186/s13063-024-07965-6.
29. Tasa T, et al. DosOpt: a tool for personalized bayesian dose adjustment of vancomycin in neonates. Ther Drug Monit. 2017;39(6):604–13. https://doi.org/10.1097/FTD.0000000000000456.
30. Colin PJ, et al. Vancomycin pharmacokinetics throughout life: results from a pooled population analysis and evaluation of current dosing recommendations. Clin Pharmacokinet. 2019;58(6):767–80. https://doi.org/10.1007/s40262-018-0727-5.
31. Ulldemolins M, et al. Piperacillin population pharmacokinetics in critically ill patients with multiple organ dysfunction syndrome receiving continuous venovenous haemodiafiltration: effect of type of dialysis membrane on dosing requirements. J Antimicrob Chemother. 2016;71(6):1651–9. https://doi.org/10.1093/jac/dkv503.
32. Dhaese SAM, et al. Saturable elimination of piperacillin in critically ill patients: implications for continuous infusion. Int J Antimicrob Agents. 2019;54(6):741–9. https://doi.org/10.1016/j.ijantimicag.2019.08.024.
33. West GB, Brown JH, Enquist BJ. A general model for the origin of allometric scaling laws in biology. Science. 1997;276(5309):122–6. https://doi.org/10.1126/science.276.5309.122.

34. Eleveld DJ, et al. A general purpose pharmacokinetic model for propofol. Anesth Analg. 2014;118(6):1221–37. https://doi.org/10.1213/ANE.0000000000000165.
35. Junge W, et al. Determination of reference intervals for serum creatinine, creatinine excretion and creatinine clearance with an enzymatic and a modified Jaffe method. Clin Chim Acta. 2004;344(1–2):137–48. https://doi.org/10.1016/j.cccn.2004.02.007.
36. Eleveld DJ, et al. An allometric model of remifentanil pharmacokinetics and pharmacodynamics. Anesthesiology. 2017;126(6):1005–18. https://doi.org/10.1097/ALN.0000000000001634.
37. Johansson AM, et al. A population pharmacokinetic/pharmacodynamic model of methotrexate and mucositis scores in osteosarcoma. Ther Drug Monit. 2011;33(6):711–8. https://doi.org/10.1097/FTD.0b013e31823615e1.
38. Bergstrand M, et al. Prediction-corrected visual predictive checks for diagnosing nonlinear mixed-effects models. AAPS J. 2011;13(2):143–51. https://doi.org/10.1208/s12248-011-9255-z.
39. Dosne AG, Bergstrand M, Karlsson MO. An automated sampling importance resampling procedure for estimating parameter uncertainty. J Pharmacokinet Pharmacodyn. 2017;44(6):509–20. https://doi.org/10.1007/s10928-017-9542-0.
40. Guidance for Industry: Content and Format for Geriatric Labeling. 2001, United States Food and Drug Administration.
41. Pediatric expertise for advisory panels: guidance for industry and FDA Staff. 2003, United States Food and Drug Administration.
42. Guideline on good pharmacovigilance practices (GVP): Product- or Population-Specific Considerations IV: Paediatric population. 2018, European Medicines Agency.
43. Reflection paper on the pharmaceutical development of medicines for use in the older population. 2020, European Medicines Agency.
44. Gin A, et al. Piperacillin-tazobactam: a beta-lactam/beta-lactamase inhibitor combination. Expert Rev Anti Infect Ther. 2007;5(3):365–83. https://doi.org/10.1586/14787210.5.3.365.
45. Felton TW, et al. Pulmonary penetration of piperacillin and tazobactam in critically ill patients. Clin Pharmacol Ther. 2014;96(4):438–48. https://doi.org/10.1038/clpt.2014.131.
46. Taccone FS, et al. Insufficient beta-lactam concentrations in the early phase of severe sepsis and septic shock. Crit Care. 2010;14(4):R126. https://doi.org/10.1186/cc9091.
47. Tsai D, et al. Pharmacokinetics of piperacillin in critically ill Australian indigenous patients with severe sepsis. Antimicrob Agents Chemother. 2016;60(12):7402–6. https://doi.org/10.1128/AAC.01657-16.
48. Weinelt FA et al. A joint pharmacokinetic model of piperacillin/tazobactam including mechanistic renal clearance in critically ill patients. In: PAGE 2019. 2019. Stockholm, Sweden
49. Wallenburg E, et al. An integral pharmacokinetic analysis of piperacillin and tazobactam in plasma and urine in critically ill patients. Clin Pharmacokinet. 2022;61(6):907–18. https://doi.org/10.1007/s40262-022-01113-6.
50. Barker CIS, et al. The Neonatal and Paediatric Pharmacokinetics of Antimicrobials study (NAPPA): investigating amoxicillin, benzylpenicillin, flucloxacillin and piperacillin pharmacokinetics from birth to adolescence. J Antimicrob Chemother. 2023;78(9):2148–61. https://doi.org/10.1093/jac/dkad196.
51. Li Z, et al. Population pharmacokinetics of piperacillin/tazobactam in neonates and young infants. Eur J Clin Pharmacol. 2013;69(6):1223–33. https://doi.org/10.1007/s00228-012-1413-4.
52. Wen S, et al. OAT1 and OAT3 also mediate the drug-drug interaction between piperacillin and tazobactam. Int J Pharm. 2018;537(1–2):172–82. https://doi.org/10.1016/j.ijpharm.2017.12.037.
53. Wu W, Bush KT, Nigam SK. Key role for the organic anion transporters, OAT1 and OAT3, in the in vivo handling of uremic toxins and solutes. Sci Rep. 2017;7(1):4939. https://doi.org/10.1038/s41598-017-04949-2.
54. Noronha IL, et al. Glomerular filtration in the aging population. Front Med (Lausanne). 2022;9: 769329. https://doi.org/10.3389/fmed.2022.769329.
55. Maarbjerg SF, et al. Continuous infusion of piperacillin-tazobactam significantly improves target attainment in children with cancer and fever. Cancer Rep (Hoboken). 2022;5(10): e1585. https://doi.org/10.1002/cnr2.1585.
56. Assefa GM, et al. What are the optimal pharmacokinetic/pharmacodynamic targets for beta-lactamase inhibitors? A systematic review. J Antimicrob Chemother. 2024;79(5):946–58. https://doi.org/10.1093/jac/dkae058.
57. Bentley DJ. Comment on: 'What are the optimal pharmacokinetic/pharmacodynamic targets for beta-lactamase inhibitors? A systematic review. J Antimicrob Chemother. 2024;79(8):2081–2. https://doi.org/10.1093/jac/dkae202.
58. Komuro M, et al. Inhibition of the renal excretion of tazobactam by piperacillin. J Antimicrob Chemother. 1994;34(4):555–64. https://doi.org/10.1093/jac/34.4.555.
59. Wise R, et al. Pharmacokinetics and tissue penetration of tazobactam administered alone and with piperacillin. Antimicrob Agents Chemother. 1991;35(6):1081–4. https://doi.org/10.1128/AAC.35.6.1081.

Authors and Affiliations

Daming Kong[1] · Jason A. Roberts[2,3,4,5] · Jeffrey Lipman[5,6] · Fabio Silvio Taccone[7] · Michael Cohen-Wolkowiez[8] · Fekade B. Sime[2] · Danny Tsai[2,9,10] · Pieter A. J. G. De Cock[11,12,13,14] · Sutep Jaruratanasirikul[15] · Sofie A. M. Dhaese[16] · Andrew A. Udy[17] · Timothy W. Felton[18,19] · Robin Michelet[20] · Céline Thibault[21,22] · Jeroen V. Koomen[1] · Douglas J. Eleveld[1] · Michel M. R. F. Struys[1,12] · Jan J. De Waele[23,24] · Pieter J. Colin[1] · PIP/TAZ Consortium

✉ Pieter J. Colin
p.j.colin@umcg.nl

[1] Department of Anesthesiology, University of Groningen, University Medical Center Groningen, P. O. Box 30001, 9700 RB Groningen, The Netherlands

[2] University of Queensland Centre for Clinical Research, Faculty of Medicine, University of Queensland, Herston, Brisbane, QLD, Australia

[3] Pharmacy Department, Royal Brisbane and Women's Hospital, Brisbane, Australia

[4] Department of Intensive Care, Royal Brisbane and Women's Hospital, Brisbane, Australia

[5] Nimes University Hospital, University of Montpellier, Nimes, France

[6] Jamieson Trauma Institute, Royal Brisbane and Women's Hospital, University of Queensland, Brisbane, Australia

[7] Department of Intensive Care, Hôpital Universitaire de Bruxelles (HUB), Université Libre de Bruxelles (ULB), Brussels, Belgium

[8] Department of Pediatrics, Duke University, Durham, NC, USA

[9] Department of Intensive Care Medicine, Alice Springs Hospital, Alice Springs, NT, Australia

[10] Pharmacy Department, Alice Springs Hospital, Alice Springs, NT, Australia

[11] Department of Pharmacy, Ghent University Hospital, De Pintelaan 185, 9000 Ghent, Belgium

[12] Department of Basic and Applied Medical Sciences, Ghent University, De Pintelaan 185, 9000 Ghent, Belgium

[13] Department of Paediatric Intensive Care, Ghent University Hospital, De Pintelaan 185, 9000 Ghent, Belgium

[14] Division of Pharmacology, Leiden Academic Centre for Drug Research, Einsteinweg 55, 2333 CC Leiden, The Netherlands

[15] Department of Medicine, Faculty of Medicine, Prince of Songkla University, Hat Yai, Songkhla 90110, Thailand

[16] Department of Nephrology and Infectious Diseases, Saint John's Hospital, Ruddershove 10, 8000 Bruges, Belgium

[17] Department of Intensive Care and Hyperbaric Medicine, The Alfred Hospital, Commercial Road, Melbourne, VIC 3181, Australia

[18] Division of Infection, Immunity to Infection and Respiratory Medicine, Faculty of Biology, Medicine and Health, The University of Manchester, Manchester, UK

[19] Acute Intensive Care Unit, Manchester University NHS Foundation Trust, Manchester, UK

[20] Department of Clinical Pharmacy and Biochemistry, Institute of Pharmacy, Freie Universität Berlin, Berlin, Germany

[21] Department of Pediatrics, CHU Sainte-Justine, Montreal, Canada

[22] Research Center, CHU Sainte-Justine, Montreal, Canada

[23] Department of Internal Medicine and Pediatrics, Faculty of Medicine and Health Sciences, Ghent University, De Pintelaan 185, 9000 Ghent, Belgium

[24] Department of Intensive Care Medicine, Ghent University Hospital, De Pintelaan 185, 9000 Ghent, Belgium